A Monte Carlo simulation of nanoscale magnetic particle morphology and magnetization

Ziyun Di, Dongchen Zhang, and Xianfeng Chen[a)]
Department of Physics, The State Key Laboratory on Fiber Optic Local Area Communication Networks and Advanced Optical Communication Systems, Shanghai Jiao Tong University, Shanghai 200240, China

(Received 23 June 2008; accepted 17 September 2008; published online 11 November 2008)

A model based on Monte Carlo technique is applied to investigating the superparamagnetic magnetite (Fe_3O_4) colloidal nanocrystal clusters (CNCs) proposed by Ge *et al.* [Nano Lett. **7**, 3203 (2007)]. In other words, the model investigates the following three aspects of CNCS: the morphology of magnetic particles, the formation of field-induced chainlike patterns, and the induced evolution of the magnetization processes. It is shown that the parameters such as diameter, surfactant molecules per unit, and volume concentration of the magnetic fluid are significant factors that enable one to efficiently manipulate the morphology and magnetization process, which eventually leads to the efficient control of the fabrication and multiple applications. The experiment results also evidenced the presence of this self-assembled chain structures. © *2008 American Institute of Physics*. [DOI: 10.1063/1.3009975]

I. INTRODUCTION

Fabrication of the various forms of nanostructured matter is at the heart of modern nanoscience.[1] Requiring different fabrication methods, various liquid, gaseous, solid, and colloidal systems have been used as the precursor medium for myriad nanoscale assemblies. As one of these nanostructured magnetic materials, magnetic fluid is a stable colloid consisting of finely divided single-domain magnetic nanoparticles (usually 3–15 nm in diameter) coated with a molecular layer of dispersant, and these nanoparticles disperse in a suitable liquid carrier.[2] Its potential applications to optical devices have been proposed, such as optical switches, tunable optical gratings, and optical tunable modulator.[3–6] Impressive progress has been made in the synthesis of magnetic colloidal nanocrystals with well-defined structures. Sun and Murray systematically synthesized and isolated nearly monodisperse nanocrystal samples ranging in size from 2 to 11 nm while maintaining better than a 7% standard deviation in diameter. The synthesized cobalt particles are each a single crystal with a complex cubic structure related to the beta phase of elemental manganese (ε-Co). Deposition of these uniform cobalt particles on solid substrates by evaporation of the carrier solvent will result in the spontaneous assembly of two-dimensional and three-dimensional magnetic superlattices (colloidal crystals).[7] Puntes *et al.* have developed a method of producing high-quality magnetic colloidal dispersions by the rapid pyrolysis of cobalt carbonyl in an inert atmosphere to produce monodispersed, stabilized, defect-free ε -cobalt nanocrystals with spherical shapes and sizes ranging from 3 to 17 nm. These particles have been observed to produce two-dimensional self-assemblies when evaporated at low rates in a controlled atmosphere.[8,9] Recently, Zhang *et al.* have reported a method for the preparation of polyacrylate-capped superparamagnetic magnetite (Fe_3O_4) colloidal nanocrystal clusters (CNCs) with tunable sizes from 30 to 180 nm by a high-temperature hydrolysis process,[10] which is a big step in the history of nanofabrication. Each cluster is composed of many magnetite crystallites of approximately 10 nm, thus retaining the superparamagnetic properties at room temperature.[11] It is suggested that such superparamagnetic clusters can be directly employed for constructing colloidal photonic crystals with highly tunable stop bands that can be moved across the entire visible spectral region owing to the highly charged polyacrylate-capped surfaces and the strong interaction of the magnetite CNCs with a magnetic field.[11] Because of its uniform size, anisotropic structure/shape, and the potential for magnetic control, its wide range applications in sensors and actuators, microelectromechanical systems, and photonic devices have aroused a great interest for researchers.[12–16] It is believed that all these significant applications are originated from these field induced self-assembly chain structures.[17–19] Therefore, it is imperative for researchers to fully study the difference in the properties between these clusters and the formal magnetic fluid, whether they are with the magnetic field or not.

It is reported that molecular dynamic simulations are applied to investigating the silica-coated cobalt nanoparticles when driven by a weak external magnetic field. By taking magnetic dipolar forces into account, silica-coated cobalt nanoparticles were found to organize into self-assembled chains structures.[20] On the other hand, Chantrell *et al.*[21] have developed a method based on Monte Carlo technique, which was proposed by Metropolis *et al.*[22] to investigate the effects of magnetostatic and repulsive interparticle interactions on the properties of a magnetic fluid. With the use of this Monte Carlo technique, we will discuss here self-assembled chain structures, magnetization processes, and morphology differences. Our experiment results also evidenced the presence of these self-assembled chain structures. The results of our re-

[a)]Author to whom correspondence should be addressed. Electronic mail: xfchen@sjtu.edu.cn.

search suggest a viable way to improve the related magnetic structure nanofabrication processes, which will be helpful to the future application of these "magnetic fluid."

II. MODEL AND NUMERICAL METHOD

Magnetostatic energies and dipolar interactions play a fundamental role in the mechanisms of patterned films and nanoelements, which are considered as candidates for the implementation of recording media.[23,24] The formation of agglomerates in magnetic fluids has been investigated by using the Monte Carlo technique developed by Metropolis *et al.*[22] The calculation is based on the Monte Carlo method, which is used to predict that the configurations of the particles in the magnetic fluid under the magnetic field and how the configurations vary with the field and other parameters. Here, a two-dimensional system of N particles of diameter D in a square of the length L is considered and the position of the particles can be specified by the coordinates (x, y, θ). The magnetostatic interaction energy was calculated by using Eq. (1), depending on the center to center distance.

$$E_m = -\sum_{j\neq i} (M_s^2\pi^2 D^6/36R_{ij}^3)[2\cos(\theta_i-\varphi)\cos(\theta_j-\varphi) - \sin(\theta_i-\varphi)\sin(\theta_j-\varphi)] \quad (R_{ij}<5D), \tag{1}$$

where M_s is the saturation magnetization of the bulk material and R_{ij} is the center to center distance between particles i and j. θ_i and θ_j are the angles between the magnetic moment and the magnetic field for particles i and j, respectively, and φ is the angle between the magnetic field and the line joining the center of the particles. In this case, the magnetic field is uniform in the film region, so the induced energy of the particle could be determined by the magnetic field, which can be described with the following equation:

$$E_h = -\mu_0\mu H\cos\theta_i, \tag{2}$$

where μ_0 is the permeability in vacuum and $\mu=\pi M_s D^3/6$ is the magnetic moment of the particle. Meanwhile, the energy due to the short range Van der Waals forces, caused by the surfactant coating, is expressed in the following pattern:

$$E_r = \sum \frac{\pi D^2 N' kT}{4}\left[2-\frac{(h+2)}{b}\ln\frac{(1+b)}{(1+h/2)}-h/b\right] \quad (R_{ij}\leq(D+2\delta)) \tag{3}$$

where δ is the thickness of the surfactant coating, N' is the number of surfactant molecules per unit area of the particle surface, $h=(2R_{ij}/D-2)$, and $b=2\delta/D$.

Therefore, the energy E of a given particle is the contribution of the above three energy formats. Basically, the essence of the Monte Carlo technique is to discuss the energy change ΔE when the coordinates of one particle are moved at random by a small amount. Then the comparison begins. If the energy difference $\Delta E=E_i'-E_i$ is negative, the particle is allowed to move. Otherwise, a random number $X(0\leq X\leq 1)$ is generated to compare with $\exp(-\Delta E/kT)$, which is regarded as the chance of the particle to overcome the thermal energy potential barrier, where k is the Boltzmann constant and T is the temperature. In such a condition, if $\exp(-\Delta E/kT)>X$, the move is encouraged. Otherwise, the move is forbidden and the particle is returned to its original position. In this procedure, all the N particles experienced this kind of movement and comparison in turn. This procedure is repeated until the magnetism converges to an essential value. After a sufficiently large number of moves, the self-assembled configuration is observed.

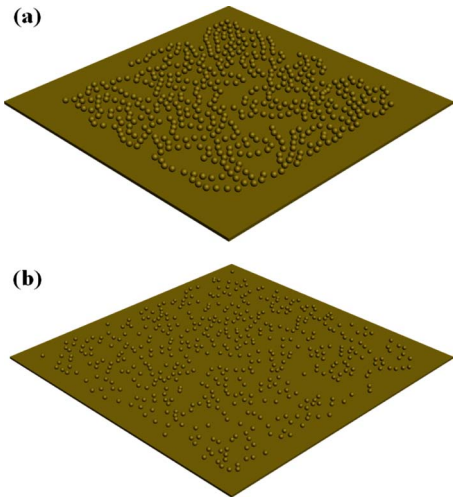

FIG. 1. (Color online) Simulation results of Fe_3O_4 nanoparticles in zero field, the particle diameter is (a) 120nm (CNCs) and (b) 10nm.

III. RESULTS AND DISCUSSION

The simulated self-organized structures with no external field are shown in Fig. 1 with the magnetic Fe_3O_4 particle diameters of 120 nm (CNCs) and 10 nm, respectively, at a temperature of $T=300$ K. One can notice that the resulting patterns will thus feature quite different surface morphologies, with somewhat unwelcome buildups in Fig. 1(a). This phenomenon can be explained in such a way that the dependence of the morphology on N' between the regular particles and the larger diameter ones (CNCs) is different. Indeed, comparing Eqs. (1) and (3), one can notice that $E_m\propto D^6$ and $E_r\propto D^2$. Apparently, the presence of a larger diameter will result in a remarkable enhancement of the magnetostatic interaction energy, which gives rise to the self-organized structures shown in Fig. 1(a). Thus, different scales of the diameter with the same value of N' will result in a quite different behavior of the configuration with no external field. Therefore, the N' can be regarded as another useful control parameter of the fabrication of the ordered nanostructures.

Figure 2(a) illustrates the initial randomly created coordinates of 500 particles with its magnetic Fe_3O_4 particle diameter of 120 nm (CNCs) and the volume concentration of 12%. Figure 2(b) features a self-assembled chain pattern generated at 600 Oe field, with the same parameters, as shown in Fig. 2(a). This pattern appears because of the following physical mechanism: with the magnetic moment of the particle aligns itself with the external magnetic field, the particle drags the surrounding magnetic particles. If the particles are close enough, their head-to-tail dipole-dipole attraction overcomes the repulsion promoted by the surfactant coating, which is a necessary for the magnetic fluid to remain

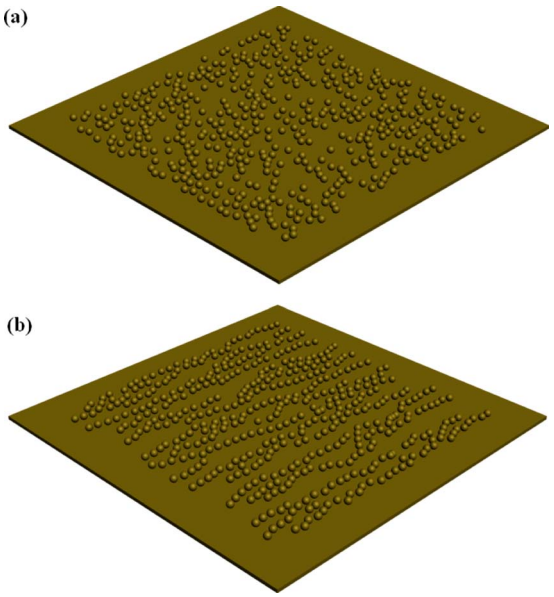

FIG. 2. (Color online) (a) The initial randomly created coordinates of 500 particles with its diameter of 120 nm (CNCs) and the volume concentration of 12%. (b) Simulation results of 120 nm (CNCs) Fe_3O_4 nanoparticles self-assembled chain pattern generated at 600 Oe field with the same volume concentration as shown in (a).

in long term stability. A chain of particles is then formed with magnetic moment pointing along the chain, with a zero angle between the field and the line joining the center of the particles.

The sample we have used here is provided by Research Centre of Micro/Nano Science and Technology of Shanghai Jiao Tong University. The sample is the hydrophilic composite nanospheres with an average diameter of 120 nm (CNCs), and its volume concentration of 2.5%. The fluid was then injected into a 7-μm-thick glass cell to form a film. An optical microscope was used to record the structures in the film. From Fig. 3, one can find out that these magnetic chains are distributed at random in the glass cell. With the increase of the field strength, more and more chains appear with a closer distance between each other. Therefore, a rapid shift of the stop band is observed in response to the increase of the field strength, corresponding to the decrease of the interplanar spacing. As estimated by the Bragg's law ($\lambda = 2nd \sin\theta$, where λ is the diffraction wavelength, n is the refractive index of water, d is the lattice plane spacing, and $\theta = 90°$ is the Bragg angle), such superparamagnetic clusters in a mag-

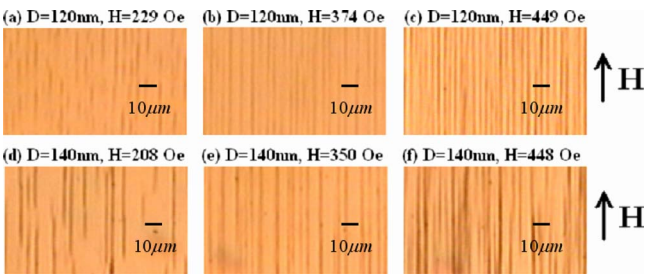

FIG. 3. (Color online) Experimental structural patterns in the magnetic fluid under the field of (a) 229 Oe, (b) 374 Oe, (c) 449Oe, (d) 208 Oe, (e) 350 Oe, and (f) 448 Oe. The particle diameter is 120 nm (CNCs) in (a)–(c), and 140 nm (CNCs) in (d)–(f).

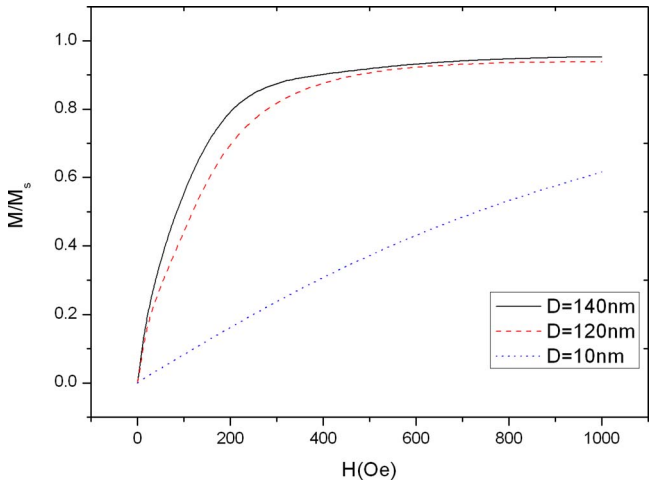

FIG. 4. (Color online) Induced magnetization curves vs magnetic field with the same volume concentration, the particle diameter is 140 nm (CNCs), 120 nm (CNCs), 10 nm, respectively.

netic field can be directly employed for constructing colloidal photonic crystals with highly tunable stop bands that can be moved across the entire visible spectrum.[11]

On the other hand, another characteristic of these systems that we are interested in is the reduced magnetization of two kinds of magnetic fluid, which can be analyzed by studying the evolution of its energy minimum as a function of the field

$$M/M_s = \lim\left[\sum_{k=1}^{n} (\cos\theta_k)/n\right], \tag{4}$$

where M and M_s are the magnetizations of the system in a field H and at saturation respectively, θ_k is the value of θ at the end of move k, and n is the total number of moves.

The curves in Fig. 4 suggest the distribution of the magnetizations over the magnetic fields depends on the particle diameter. It is notable that in both the cases of diameter 120 and 140 nm, the magnetization value increases steeply in the range of 0–300 Oe, and then increases smoothly in the subsequent field range (300 Oe$<$H$<$400 Oe). Finally it will get saturated when $H>400$ Oe. Interestingly, the magnetization curve of the 10 nm case is continuously increasing even in the large field area, which shows some signs of difference compared with the others. In this figure, the approach to saturation is a strong function of particle size. The 140 nm diameter particles are 95% saturated in a magnetic field of 500 Oe while the 10 nm diameter particles are only about 40% saturated under the same condition. Physically, this is attributed to an excellent enhancement in the magnetostatic interaction energy in the larger diameter situation, which strongly affects the alignment of the magnetic moment into the field direction. The easier this trend could be, the more quickly it will reach its saturation magnetization.

Figure 5 displays the dependence of the magnetization on the field, with the volume concentration as a parameter. Such a dependence accounts for the fact that the effect of induced magnetization would be weakened for the low particle densities at the lower field range (0–300 Oe) and be-

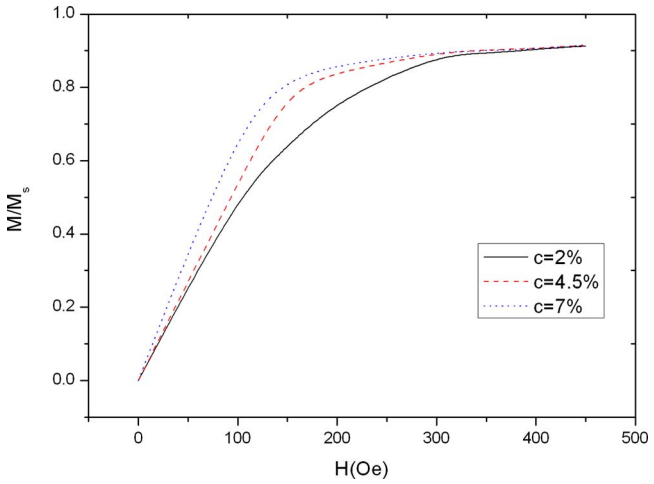

FIG. 5. (Color online) Induced magnetization curves vs magnetic field with the same the particle diameter of 120 nm (CNCs), volume concentration c is 7%, 4.5%, and 2%, respectively.

come saturated at later range. It appears that the higher volume concentration is more pronounced in the lower field region.

Therefore, it has been clearly demonstrated that the field-induced magnetization properties of superparamagnetic magnetite CNCs show some signs of advantage, but it is also accompanied with the higher request of the fabrication techniques when talking to the particle morphology.

IV. CONCLUSION

In conclusion, a Monte Carlo technique is applied to analyzing the morphology of the nanostructured two magnetic fluid systems, whether they are with the magnetic field or not. It is found that the self-organized structures differ greatly due to the remarkable change of the magnetostatic interaction energy because of the difference of the diameters of the particles. Additionally, in this paper, the comparisons of the evolutions of the magnetization processes and magnetic moments of the two systems are investigated. Our results suggest that the parameters such as diameter, surfactant molecules per unit, and volume concentration of the magnetic fluid, are significant factors that enable one to efficiently manipulate the magnetization process, eventually leading to the efficient control of the fabrication and multiple applications. In addition, our experiment results evidence the presence of this self-assembled chain structures. This approach may represent a helpful result toward the important link between fabrication and their multiple applications.

ACKNOWLEDGMENTS

This research was supported by the National Natural Science Foundation of China (No. 10574092), the National Basic Research Program "973" of China (No. 2007CB307000), and the Shanghai Leading Academic Discipline Project.

[1]M.C. Roco, S. Williams, and P. Alivisatos, Nanotechnology Research Directions: Vision for Nanotechnology Research and Development in the Next Decade, 1999 (unpublished).
[2]R. E. Rosensweig, *Ferrohydrodynamics* (Cambridge University Press, Cambridge, 1985).
[3]Z. Di, X. Chen, S. Pu, X. Hu, and Y. Xia, Appl. Phys. Lett. **89**, 211106 (2006).
[4]S. Pu, X. Chen, L. Chen, W. Liao, Y. Chen, and Y. Xia, Appl. Phys. Lett. **87**, 021901 (2005).
[5]T. Du and W. Luo, Appl. Phys. Lett. **72**, 272 (1998).
[6]H. E. Horng, C. S. Chen, K. L. Fang, S. Y. Yang, J. J. Chieh, C. Y. Hong, and H. C. Yang, Appl. Phys. Lett. **85**, 5592 (2004).
[7]S. Sun and C. B. Murray, J. Appl. Phys. **85**, 4325 (1999).
[8]V. F. Puntes, K. M. Krishnana, and P. Alivisatos, Appl. Phys. Lett. **78**, 2187 (2001).
[9]V. F. Puntes, K. M. Krishnan, and A. Paul Alivisatos, Science **291**, 2115 (2001).
[10]T. Zhang, J. Ge, Y. Hu, and Y. Yin, Nano Lett. **7**, 3203 (2007).
[11]J. Ge, Y. Hu, and Y. Yin, Angew. Chem., Int. Ed. **46**, 7428 (2007).
[12]W. Luo, T. Du, and J. Huang, J. Magn. Magn. Mater. **201**, 88 (1999).
[13]H.-E. Horng, C. Y. Hong, W. B. Yeung, and H. C. Yang, Appl. Opt. **37**, 2674 (1998).
[14]P. C. Fannin, C. Mac Oireachtaighl, S. Odenbach, and N. Mattoussevitch, J. Phys. D **40**, 6484 (2007).
[15]E. Mosiniewicz-Szablewska, M. Safarikova, and I. Safarik, J. Phys. D **40**, 6490 (2007).
[16]P. C. Fannin, P. A. Perov, and S. W. Charles, J. Phys. D **32**, 1583 (1999).
[17]W. Luo, T. Du, and J. Huang, Phys. Rev. Lett. **82**, 4134 (1999).
[18]S. Taketomi, J. Appl. Phys. **22**, 1137 (1983).
[19]J. H. E. Promislow, A. P. Gast, and M. Fermigier, J. Chem. Phys. **102**, 5492 (1995).
[20]V. Salgueiriño-Maceira, M. A. Correa-Duarte, A. Hucht, and M. Farle, J. Magn. Magn. Mater. **303**, 163 (2006).
[21]R. W. Chantrell, A. Bradbury, J. Popplewell, and S. W. Charles, J. Appl. Phys. **53**, 2742 (1982).
[22]N. Metropolis, A. W. Rosenbluth, M. N. Rosenbluth, A. H. Teller, and E. Teller, J. Chem. Phys. **21**, 1087 (1953).
[23]O. E. Garcia, V. Naulin, A. H. Nielsen, and J. Juul Rasmussen, Phys. Rev. Lett. **92**, 165003 (2004).
[24]N. Weiss, T. Cren, M. Epple, S. Rusponi, G. Baudot, S. Rohart, A. Tejeda, V. Repain, S. Rousset, P. Ohresser, F. Scheurer, P. Bencok, and H. Brune, Phys. Rev. Lett. **95**, 157204 (2005).